Author version, to be cited as: ChemPhysChem 10.1002/cphc.201501160. VoR link: http://dx.doi.org/10.1002/cphc.201501160

Dethreading of a photoactive azobenzene-containing molecular axle from a crown ether ring: a computational investigation

Gloria Tabacchi,[a] Serena Silvi,[b] Margherita Venturi,[b] Alberto Credi*[b] and Ettore Fois*[a]

Abstract: Pseudorotaxanes formed by a dibenzo[24]crown-8 ring (**R**) and a dialkylammonium axle bearing either two *E*- or two *Z*-azobenzene units (*EE*-**A** or *ZZ*-**A**) revealed useful for the construction of light-powered molecular machines and motors, as they provide the opportunity of photocontrolling self-assembly/disassembly processes. The potential energies profiles for the dethreading of these complexes have been investigated by adopting a combination of first-principles molecular dynamics, metadynamics and quantum-chemical geometry optimization approaches. While the dethreading of the *EE*-**A** axle is associated with a monotonic energy increase, for that of the *ZZ*-**A** axle a transition state and an intermediate structure, in which the components are still threaded together, are found. The rate determining step for the dethreading of the *ZZ* axle has a higher energy barrier than that of the *EE* axle, in agreement with the experimental kinetic data. Moreover, the results suggest that the elliptic shape of the ring cavity is important for discriminating between the *E* and *Z* terminal azobenzene during dethreading.

Introduction

Rotaxanes are entities composed minimally of an axle-type molecule surrounded by a macrocycle and bearing bulky groups (stoppers) at both extremities, so that the molecular ring and axle components are mechanically interlocked.[1,2] If the stoppers are absent, a chemical equilibrium is established between the disassembled and assembled (that is, threaded) molecular components. Rotaxanes and pseudorotaxanes are interesting for the construction of molecular machines,[3,4] because the modulation of the intercomponent interactions by external signals can lead to stimuli-controlled large-amplitude movements of the molecular components.[5]

The rotaxane or pseudorotaxane character of a given macrocycle-axle pair is determined by the threading-dethreading rate constants which, in turn, depend on the temperature and the energy barriers associated with these processes.[6] Indeed, temperature-dependent threading-dethreading processes are at the basis of the well known and widely used slippage methodology for the synthesis of rotaxanes.[7] In recent years, ring-axle molecular systems in which the threading-dethreading kinetics can be changed by adjusting the corresponding energy barriers through external stimulation at constant temperature have been reported.[8,9] These studies are important for the development of molecular motors, as the control of the transition rates between different states of the device is the key for the implementation of ratchet-type mechanisms.[10]

In a previous study[9,11] we investigated the threading-dethreading equilibria of the dibenzo[24]crown-8 ring **R** with axles *EE*-**A** and *ZZ*-**A**, composed of a dialkylammonium recognition site equipped respectively with two *E*-azobenzene or two *Z*-azobenzene end units (Scheme 1). Taking advantage of the well known azobenzene photoisomerization,[12] the *EE*-**A** and *ZZ*-**A** components can be reversibly interconverted into one another with light irradiation and/or heating (Scheme 1).[9]

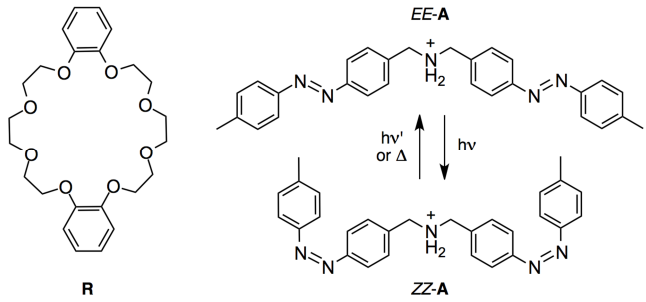

Scheme 1. Structural formulas of the investigated ring (**R**) and axle (**A**) compounds, and light and heat-induced interconversion between the *EE* and *ZZ* configurational isomers of the axle.

In such experiments, the equilibrium ($\Delta G°$) and kinetic ($\Delta G^{\neq}$) properties of the threaded complexes [**R**⊃*EE*-**A**] and [**R**⊃*ZZ*-**A**] were experimentally determined by ^{1}H NMR spectroscopy in acetonitrile at 298 K. It was found that the thermodynamic stability of the [**R**⊃*EE*-**A**] complex ($\Delta G°_{EE}$ = –3.9 kcal mol^{-1}) is slightly higher than that of the [**R**⊃*ZZ*-**A**] one ($\Delta G°_{ZZ}$ = –3.5 kcal mol^{-1}). Remarkably, the self-assembly kinetics of **R** with the *EE*-**A** axle is much faster than with the *ZZ*-**A** axle, both for the threading ($\Delta G^{\neq}_{EE}$ = 15 kcal mol^{-1}, $\Delta G^{\neq}_{ZZ}$ = 20.9 kcal mol^{-1}) and the dethreading processes ($\Delta G^{\neq}_{EE}$ = 19.3 kcal mol^{-1}, $\Delta G^{\neq}_{ZZ}$ = 24.5 kcal mol^{-1}).[11]

As a matter of fact under the conditions employed, the photoisomerization of the *E*-azobenzene units of the axle to the *Z* form slows down the threading and dethreading rate constants by more than four orders of magnitude. In other words, [**R**⊃*EE*-**A**] is a genuine pseudorotaxane whereas [**R**⊃*ZZ*-**A**] behaves as a rotaxane. In successive studies, these features were exploited in a modified system to achieve the chemically- and light-controlled relative unidirectional transit of the ring along the axle[11] and, eventually, to construct the first example of an artificial autonomous molecular pump powered by light.[13,14]

The scope of the present work is to investigate the reasons for the significant differences in the thermodynamic and kinetic behaviour of the two threaded complexes, which is at the basis

[a] Dr. G. Tabacchi, Prof. E. Fois
Dipartimento di Scienza ed Alta Tecnologia and INSTM
Università dell'Insubria
Via Valleggio 11, I-22100 Como, Italy
E-mail: ettore.fois@uninsubria.it

[b] Dr. S. Silvi, Prof. M. Venturi, Prof. A. Credi
Photochemical Nanosciences Laboratory and Interuniversity Center for the Chemical Conversion of Solar Energy
Dipartimento di Chimica "G. Ciamician"
Università di Bologna
Via Selmi 2, I-40126 Bologna, Italy
E-mail: alberto.credi@unibo.it

Supporting information (SI) for this article is given via a link at the end of the document.

of the above mentioned light-powered molecular devices.[11,13,14] This is not a trivial problem, because the transformation between the *E* and *Z* isomers brings about remarkable variations both in the geometrical and electronic properties of the azobenzene moiety.[12] Here we report the results of computational investigations in which structural quantum chemical calculations, driven by first principles molecular dynamics and metadynamics sampling, are employed to study the interactions between the ring and axle components as a function of the degree of dethreading.

Results

As discussed in the Introduction, the experimental results obtained in acetonitrile at 298 K by ^{1}H NMR spectroscopy[9,11] revealed that (i) the [**R**⊃*EE*-**A**] complex is more stable than the [**R**⊃*ZZ*-**A**] one, and (ii) the formation and the disassembly of the complex with **R** are much faster for the *EE*-**A** than for the *ZZ*-**A** axle. A first step towards the understanding of the different behaviour of the *EE* and *ZZ* axles, and our main objective in this work, is the study of the potential energy of interaction in the ring-axle pair at different stages of the entrance of the axle into, or the exit of the axle from, the cavity of the ring. Elucidating the specific role of the ring-axle interactions in these processes – which are still unknown and presumably very complex at the molecular level – is definitely not straightforward, because solvent molecules are involved as well. Therefore, to disentangle the effects of the interactions between the molecular components of the pseudorotaxanes from those pertaining to interactions with solvent molecules, here we decided to focus our efforts solely on the exit (i.e., dethreading) process. This choice was based on the reasoning that, whereas the solvent plays a key role in the threading process, its influence should be far less important on the potential energy profile of the dethreading for the following reasons.

The dethreading process of a generic pseudorotaxane [**R**⊃**A**] involves a displacement reaction where, e.g., a (few) solvent molecule(s) **S** replace(s) a generic cationic axle **A**:

$$[\mathbf{R}\supset\mathbf{A}] + \mathbf{S} \rightarrow [\mathbf{R}\supset\mathbf{S}] + \mathbf{A} \quad (1)$$

The counteranion of the axle is not explicitly taken into consideration in this mechanism, for reasons that are explained in the Experimental Section. Formally, the displacement reaction shown in eq. (1) can be broken down in the following two processes:

$$[\mathbf{R}\supset\mathbf{A}] \rightarrow \mathbf{R} + \mathbf{A} \quad (2)$$

$$\mathbf{R} + \mathbf{S} \rightarrow [\mathbf{R}\supset\mathbf{S}] \quad (3)$$

In order to gather insight on the potential energy surface associated with the exit of the axle as a function of the axle structure, we focused our attention exclusively on the reaction represented in eq. (2). A rationale of this approach is that the solvent molecules cannot occupy the cavity of the ring until the pseudorotaxane is disassembled, namely until the axle is completely out of the ring. On this basis, it is reasonable to argue that the entrance of solvent molecules following the exit of the axle should occur essentially in the same way for the two isomers, that is, independently on the configuration (*EE* or *ZZ*) of the axle. In other words, we assume that relative differences between the potential energy surfaces describing the dethreading process of the *EE* and *ZZ* axles should be caused mainly by the structure of the axle itself. Under this assumption, we modeled only the dethreading reaction (eq. (2)) and we considered solely relative energy differences between the dethreading processes of the [**R**⊃*EE*-**A**] and [**R**⊃*ZZ*-**A**] complexes.

It should also be noticed that the activation barriers measured experimentally[9,11] are activation free energies ($\Delta G^{\neq}$), while our calculations can provide reasonable predictions of the activation potential energies ($\Delta E^{\neq}$). Therefore, in order to have a meaningful comparison with the experimental data, we will discuss relative variations of $\Delta E^{\neq}$ ($\Delta\Delta E^{\neq}$), namely, the difference between the $\Delta E^{\neq}$ values calculated for the dethreading of the two complexes. These quantities shall be compared with the corresponding $\Delta\Delta G^{\neq}$ values, with the assumption that the energetic contributions are predominant and entropy variations are mainly due to the microscopic behavior of solvent molecules, that can be considered similar in the *EE* and *ZZ* cases.

The first step in our computational strategy is to obtain the minimum energy structure of the composite systems ([**R**⊃*EE*-**A**] and [**R**⊃*ZZ*-**A**]) and of the separate components **R**, *EE*-**A** and *ZZ*-**A**. The graphical representations of the optimized geometries of these species resulting from the structural quantum chemical calculations are shown in Figure 1. In the case of the ring **R**, two stable structures were obtained: one with a chair conformation (Figure 1, top) and another, less stable by 1.5 kcal mol^{-1}, with a boat conformation. Interestingly, the cavity of host **R** is not circular but elliptical, with the long axis lying along the direction that connects the two aromatic rings.

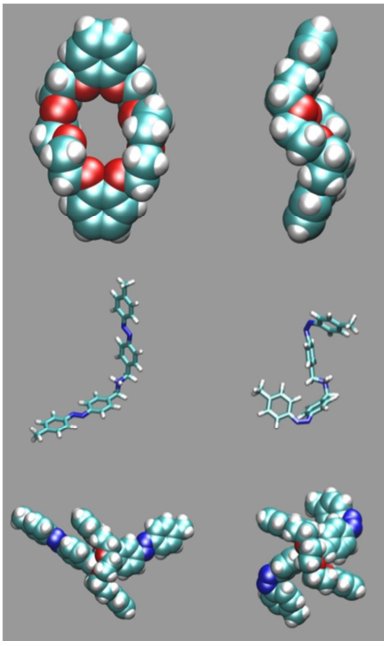

Figure 1. Representation of the optimized structures resulting from the structural quantum chemical calculations. Top: two views of the ring (dibenzo[24]crown-8) **R**. Center: stick representation of the axle in the *EE* (left) and *ZZ* (right) configuration. Bottom: [**R**⊃*EE*-**A**] (left) and [**R**⊃*ZZ*-**A**] (right) complexes. Atom colors code: C, cyan; N, blue; O, red; H, white.

We found that the [**R**⊃*EE*-**A**] structure is more stable than the [**R**⊃*ZZ*-**A**] one by about 4 kcal mol^{-1} (MP2 energies), as the binding energies amount to 60 and 56 kcal mol^{-1} for the *EE* and *ZZ* adducts, respectively. The corresponding values calculated with the PBE-Grimme functional and plane wave basis set are 60 and 57 kcal mol^{-1}, respectively, in good agreement with the previous data. The high values of the calculated binding energies stem from the fact that they are relative to the process in eq. (2) and therefore refer to the asymptotic limit of the non-interacting axle and ring, in vacuum. In all cases, irrespective of the theoretical approach adopted, the minimum energy structure of the adducts corresponds to a pseudorotaxane geometry with the ammonium protons engaged in hydrogen-bonding interactions with the oxygen atoms of the crown ether. Interestingly, and in line with experimental data obtained for similar (pseudo)rotaxanes,[15] also a proton of one CH_2 group adjacent to the ammonium center is weakly interacting with an oxygen atom of the ring, as deduced from the interatomic distances (2.38 and 2.30 Å, respectively, for the *EE* and *ZZ* complexes). Moreover, in the minimum energy structures of both complexes, the ring adopts the chair conformation.

In order to gather useful indications on the structural changes undergone by the systems along the dethreading process, instrumental for facilitating the quantitative study of the axle-ring potential energy surfaces, we simulated the escape of the axle from the ring at 300 K by combining the metadynamics approach with the first principles molecular dynamics method. The energetic profiles obtained for the exit of the axles, reported in Figure 2, show that the asymptotic value of the dethreading process is more endothermic for [**R**⊃*EE*-**A**] than for [**R**⊃*ZZ*-**A**], in line with the binding energies. From the inspection of the [**R**⊃*ZZ*-**A**] profile, however, it emerges clearly that a maximum is present in the region around the 300th metadynamics step, along with a relative minimum roughly at the 400th step.

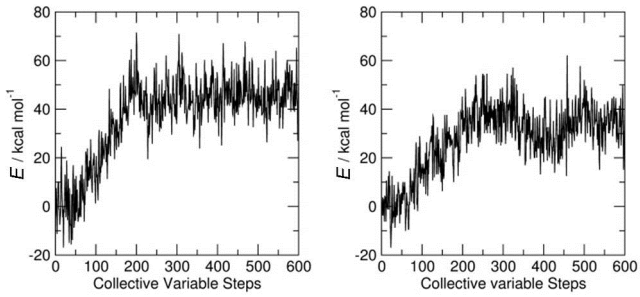

Figure 2. Energy profiles for the metadynamics simulation of the dethreading process at 300 K for the [**R**⊃*EE*-**A**] (left) and [**R**⊃*ZZ*-**A**] (right) complexes.

Starting from such a guess for the relative minimum structure, we have minimized its energy by quantum-chemical structural optimization, and the corresponding optimized geometry is reported in Figure 3, right. This structure corresponds to an intermediate along the dethreading of [**R**⊃*ZZ*-**A**] and it is characterized by a MP2+solvent+zero point energy (zpe) binding energy of 18.1 kcal mol^{-1}.

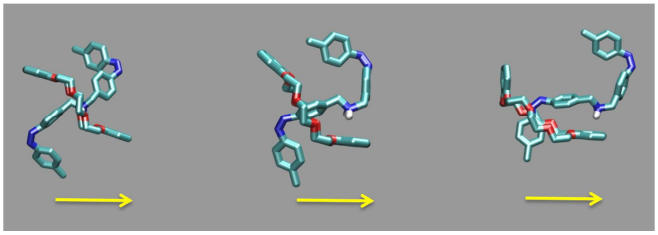

Figure 3. Graphical representations (stick models) of the minimum energy structure (left), the transition state structure (center), and the intermediate structure (right) predicted by the quantum chemical calculations for the dethreading process of [**R**⊃*ZZ*-**A**]. Only the protons of the ammonium group are represented. The arrows indicate the exit direction of the axle. Atom colors code: C, cyan; N, blue; O, red; H, white.

The presence of a stable intermediate in the dethreading process of the [**R**⊃*ZZ*-**A**] adduct implies a more complex potential energy profile with respect to the *EE* case, in which the escape of the axle occurs without relative minima (see Figure 2, left). In order to have a more detailed energetic profile for the exit of *ZZ*-**A**, we have performed quantum chemical calculations to search for a transition state (TS) in the region of the energy curve between the two minima (see Figure 2, right), corresponding to the initial state (the ring surrounds the ammonium center; Figure 3, left) and the intermediate structure (the ring surrounds a Z-azobenzene unit; Figure 3, right). The transition state, characterized by an imaginary frequency, has a

binding energy of 25.9 kcal mol^{-1} (MP2+Solvent+zpe). The structure of such a TS is represented in Figure 3 (center), while the normal mode characteristic of the TS is shown in Figure 4.

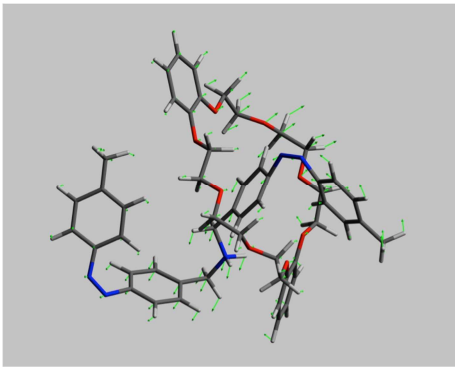

Figure 4. Graphical representation of the normal mode (green arrows) characterizing the TS structure in the dethreading process of [**R**⊃*ZZ*-**A**]. Atom colors code: C, gray; N, blue; O, red; H, white.

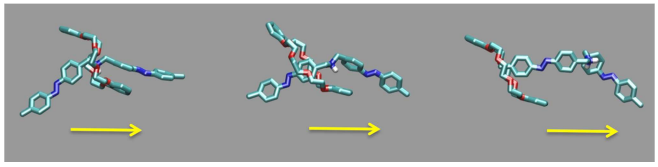

Figure 5. Snapshots from the first principles metadynamics simulation of the dethreading process of [**R**⊃*EE*-**A**] at 300 K. The arrows indicate the exit direction of the axle. Atom colors code: C, cyan; N, blue; O, red; H, white.

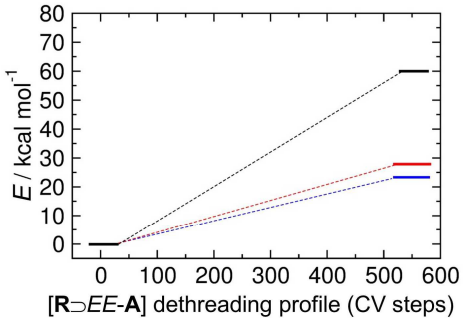

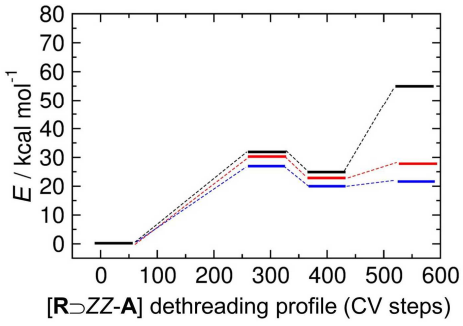

Figure 6. Schematic diagram showing the changes in the potential energy (kcal mol^{-1}) along the dethreading profile for the [**R**⊃*EE*-**A**] (top) and [**R**⊃*ZZ*-**A**] (bottom) complexes obtained via quantum chemical approaches. Black thick lines refer to calculated energies in vacuum, red thick lines refer to values including solvation energies, blue thick lines refer to values including both solvation and zero-point energies. Thin dashed lines are guides for the eye.

Table 1. Computed potential energy values (kcal mol^{-1}) for selected structures along the dethreading profile of the [**R**⊃*EE*-**A**] and [**R**⊃*ZZ*-**A**] complexes.

	Assembled[a]	Transition state[b]	Intermediate[c]	Disassembled[d]
[**R**⊃*EE*-**A**] in vacuum	0.0	[e]	[e]	60.0
[**R**⊃*EE*-**A**] incl. solv. en.	0.0	[e]	[e]	27.0
[**R**⊃*EE*-**A**] incl. solv. en. and zpe	0.0	[e]	[e]	24.4
[**R**⊃*ZZ*-**A**] in vacuum	0.0	33.0	25.0	56.0
[**R**⊃*ZZ*-**A**] incl. solv. en.	0.0	31.3	22.3	27.0
[**R**⊃*ZZ*-**A**] incl. solv. en. and zpe	0.0	25.9	18.1	21.0

[a] Structure in which the ring surrounds the ammonium center of the axle (Figures 3 and 5, left). [b] See Figure 3, center. [c] See Figure 3, right. [d] Separated axle and ring components. [e] Not observed.

As highlighted above, the *EE* pseudorotaxane disassembles without intermediate states. Figure 5 shows representative snapshots from the metadynamics simulation of the dethreading of [**R**⊃*EE*-**A**] at 300 K.

A sketch of the potential energy profiles for the dethreading of the two pseudorotaxanes is displayed in Figure 6, while the calculated values including solvation and zero-point energies are reported in Table 1. It emerges that, in agreement with our intial argument, the solvation energy plays an important role in stabilizing the disassembled molecular components after the exit of the axle, because the charged ammonium center in the uncomplexed axle lacks the stabilization brought about by the solvation-like effect exerted by the crown ether ring. On the contrary, the stabilizing effect of the solvent is far less relevant for the minima and the TS: these structures, where the axle is still well inside of the ring, are actually dominated by the interactions between the two molecular components.

Discussion

The calculations indicate a greater energetic stability of the [**R**⊃*EE*-**A**] complex (24.4 kcal mol^{-1}) with respect to the [**R**⊃*ZZ*-**A**] one (21.0 kcal mol^{-1}) in comparison with the separated molecular components, in qualitative agreement with the experimental results. However, while the *EE* axle escapes from the ring without intermediate stationary points, a transition state and a relative minimum have been detected in the dethreading of the *ZZ* axle. The TS state and the intermediate are respectively 25.9 and 18.1 kcal mol^{-1} higher in energy with respect to the [**R**⊃*ZZ*-**A**] complex. The transition state and intermediate detected along the dethreading path of the *ZZ* complex may therefore play a role in determining the different dethreading rates measured for the two pseudorotaxanes. Indeed, a higher potential energy barrier is calculated for the dethreading of [**R**⊃*ZZ*-**A**] compared to [**R**⊃*EE*-**A**], (25.9 kcal mol^{-1} *vs.* 24.4 kcal mol^{-1}), in line with the faster dethreading rate experimentally determined for the latter. The computed activation energies allow eventually to calculate $\Delta\Delta E^{\neq}$, which amounts to 1.5 kcal mol^{-1} favoring the exit of the *EE* axle. This value is in keeping with the experimental $\Delta\Delta G^{\neq}$ value of 5.2 kcal mol^{-1}.[9,11]

The transition state in the dethreading of [**R**⊃*ZZ*-**A**] is characterized by an inner phenyl moiety of the axle occupying the crown ether cavity, while the ammonium center lies approximately on the top of an aromatic ring of the crown ether (see Figure 3, center). The geometry of the intermediate structure, on the other hand, reveals a terminal phenyl moiety of the axle approaching the crown ether cavity and the charged ammonium center in close contact with an aromatic ring of the crown ether, indicating the presence of a stabilizing π-charge interaction. In this structure, one proton of the ammonium group is at 2.28 Å from a C atom belonging to a benzene ring of the crown ether. Interestingly, the phenyl rings linked to each azo group of the axle are roughly perpendicular to each other in the *ZZ* complex (Figure 3), while they are roughly parallel in the *EE* pseudorotaxane (Figure 5). Another interesting point emerges in the dethreading process of [**R**⊃*ZZ*-**A**]: the ring changes its conformation during the exit of the axle. Specifically, **R** is in the chair conformation in the stable [**R**⊃*ZZ*-**A**] complex, it adopts a boat conformation in the intermediate structure, and finally reverts to the chair conformation when the *ZZ* axle has escaped from the ring.

During the exit of the *EE* axle, the ammonium protons, like in the *ZZ* case, follow a direction which allows for a greater proximity to an aromatic unit of the ring, suggesting that also in this case a π-charge interaction is playing a role in determining the exit direction (Figure 5, center). In the case of the *EE* system, no stationary point has been detected along the dethreading path. These results may be rationalized by recalling the elliptic shape of the ring opening. As highlighted in Figure 5, the *E*-azobenzene group transits through **R** in a conformation where both its phenyl moieties lie in a plane parallel to the long axis of the macrocycle, thus allowing for a smoother dethreading process. The observation that the *EE* axle dethreads without intermediate stations, however, does not imply that the reverse process – namely, the threading of an *EE* axle in the macrocycle – is a barrierless process. Indeed, as already pointed out before, one should take into account that the entrance of an axle into the cavity of the ring requires the prior displacement of solvent molecules from the ring, which is an activated process.

Conclusions

The potential energy surface computed for the dethreading of the two investigated pseudorotaxanes evidenced a profile which is dependent on the configuration (*EE* or *ZZ*) of the axle. In the case of the [**R**⊃*EE*-**A**] complex, the energy increases monotonically as a function of the degree of dethreading and the estimated exit barrier is determined by the energetic stability (i.e., the binding energy, 24.4 kcal mol^{-1}) of the pseudorotaxane. The [**R**⊃*ZZ*-**A**] complex has a lower binding energy (21.0 kcal mol^{-1}) than its *EE* counterpart; its exit barrier, however, is higher because a transition state (25.9 kcal mol^{-1}) was found along the dethreading process, along with a relative minimum (18.1 kcal mol^{-1}). These results point therefore to different mechanisms for the dethreading of the *EE* and *ZZ* axles (a one-step process for the first one, a two-step process for the second one). Indeed, the rate determining step for dethreading of [**R**⊃*ZZ*-**A**] exhibits a larger potential energy barrier with respect to the *EE* case. Although the calculated $\Delta\Delta E^{\neq}$ (1.5 kcal mol^{-1}) is smaller that the measured $\Delta\Delta G^{\neq}$ (5.2 kcal mol^{-1}), both values indicate a slower dethreading of the [**R**⊃*ZZ*-**A**] complex. In conclusion, the present modeling study shed light, at the atomistic scale level, on the different behavior of the two complexes: it is the elliptic shape of the opening of the macrocyclic ring which is ultimately capable of discriminating between the *E* and *Z* configurations of the terminal azobenzene group of the axle in the dethreading process.

Experimental Section

Molecular dynamics. The potential energy profile for the dethreading of the axle **A** (either in the *EE* or *ZZ* configuration) from the crown ether **R** was modeled by a multi technique approach. The dethreading process was first simulated via first-principles molecular dynamics[16] augmented by metadynamics sampling.[17] The system was composed by the neutral ring **R** and by the positively charged axle (*EE*-**A** or *ZZ*-**A**). In order to keep the system electrically neutral, a iodide anion was included in the model. It should be noted that in the system studied experimentally the positively charged axles were employed as their PF_6^- salts.[9,11] The role of the counteranion was not taken into account in the present study for the following reasons: (i) since the relatively polar acetonitrile solvent prevents the formation of tight ion pairs,[18] the PF_6^- counterions should not play a role in both the equilibrium and kinetics properties of the ring-axle assembly, unless they are present in a large excess;[19] (ii) effects arising from interactions between the positively charged axle and the counteranions, if present,[20] would take place for both the EE and ZZ systems, presumably to a similar extent. The Perdew-Burke-Ernzerhof (PBE)[21] approximation to density functional theory (DFT) was used to account for the electron-electron interactions along with the Grimme correction for dispersion.[22] Ultra-soft pseudopotentials[23] were adopted for all atoms. Electronic wavefunctions were expanded in a plane-waves basis set up to a cutoff of 25 Ry (200 Ry for the electron density representation). Calculations were performed adopting periodic boundary conditions in a simulation box of size 30×30×30 Å, large enough to

minimize interactions with the periodic images. During the simulations, the iodide anion was constrained at 25 Å from the central nitrogen atom of the axle. Such a constraint value allowed for a substantial separation among the iodide and the other atoms of the systems (See Figure S1 in the Supporting Information (SI)). A time step of 5 a.u. was used for the integration of the equations of motion, together with a fictitious inertia parameter of 500 a.u. For both the [**R**⊃*EE*-**A**] and [**R**⊃*ZZ*-**A**] systems, the geometry optimization was followed by equilibration molecular dynamics runs (elapsed time: 2 ps) at 300K.

The dethreading process was induced *via* the metadynamics approach, adopting as collective variable (CV) the displacement of one of the benzene rings of the axle with respect to the oxygen atoms forming the closed ether chain of the ring. The Lagrange-Langevin dynamics for the CV evolution at 300 K with friction of 0.001 a.u. was adopted. Gaussian hills with a perpendicular width and height of respectively 0.02 and 0.002 a.u. were adopted for the production runs. With such a set-up, complete dethreading was achieved in about half a thousand metadynamics steps, amounting to roughly 120000 steps of first-principles molecular dynamics. Calculations were performed with the CPMD code.[24]

Energy Optimization. The geometries of the [**R**⊃*EE*-**A**] and [**R**⊃*ZZ*-**A**] complexes and of their components **R**, *EE*-**A** and *ZZ*-**A** were optimized adopting a diverse set of theoretical methods. First, with the same set-up adopted in the finite temperature molecular dynamics and metadynamics simulations, at regular intervals of the metadynamics trajectory we selected a configuration and minimized its energy via the simulated annealing approach. We selected geometries where at least one of the phenyl moieties of the axles was inside the crown-ether ring. The annealed structures were further optimized, in an isolated cubic box (30 Å side) without the iodide anion (See Figure S2 in SI). The minimum structures calculated with and without the iodide were consistent, indicating that no spurious effect has been introduced by including the iodide anion in the periodic-DFT simulations. These sequences of optimizations led to one minimum structure for the [**R**⊃*EE*-**A**] system, and to two minima for the [**R**⊃*ZZ*-**A**] complex. Lastly, starting from these minima, we have performed for all the investigated species structural optimization with the quantum-chemical approach, by adopting a gaussian basis set and the B3lyp functional. As an example, two representative sequences of configurations taken from optimization runs of the [**R**⊃*EE*-**A**] and [**R**⊃*ZZ*-**A**] systems are reported in Figure S3 and S4 of the SI, respectively.

The binding energies of the adducts were obtained from the difference between the total energy of the complex and the sum of the minimum energies of the isolated ring and axle components. With this quantum-chemical approach, we have performed a vibrational analysis calculation to obtain the harmonic frequencies in order to calculate the zero-point energies of the different species. In the case of the [**R**⊃*ZZ*-**A**] system, a transition state search was performed using as a guess the geometry corresponding to the 300th metadynamics step. By adopting the B3lyp optimized geometries, we have calculated energies at the MP2 level of theory. MP2 binding energies were obtained by subtracting the energies of the components (e.g., **R** and *EE*-**A**) from the energy of the complex (e.g., [**R**⊃*EE*-**A**]). Binding energies at the MP2 level were then corrected, via the counterpoise method, in order to take into account the basis set superposition error.

Solvation energies were calculated, at the MP2 level, with the Polarizable Continuum Model (PCM)[25] by adopting the acetonitrile parameters for the solvent. For the case of the dethreading of the [**R**⊃*ZZ*-**A**] system, we have also performed a transition state search, by looking for a geometry with an imaginary frequency (one negative eigenvalue). All calculations with the gaussian basis set were performed with the G09 suite of programs[26] and by adopting the D95(d,p) basis set.

Acknowledgements

This work was supported by the Italian Ministry of Education, University and Research (MIUR, PRIN 2010CX2TLM "InfoChem" project) and the University of Bologna (FARB Programme for basic research, "SLaMM" project).

Keywords: metadynamics • molecular dynamics • molecular machine • rotaxane • supramolecular chemistry

[1] J.-P. Sauvage and C. Dietrich-Buchecker (Eds.), *Molecular Catenanes, Rotaxanes and Knots: A Journey Through the World of Molecular Topology*, Wiley-VCH, Weinheim, **1999**.

[2] J. F. Stoddart, *Chem. Soc. Rev.* **2009**, *38*, 1802.

[3] V. Balzani, A. Credi, M. Venturi, *Molecular Devices and Machines – Concepts and Perspectives for the Nanoworld*, Weinheim, Wiley-VCH, Weinheim, **2008**.

[4] a) S. Erbas-Cakmak, D. A. Leigh, C. T. McTernan, A. L. Nussbaumer, *Chem. Rev.* **2015,** *115*, 10081; b) S. F. M. Van Dongen, S. Cantekin, J. A. A. W. Elemans, A. E. Rowan, R. J. M. Nolte, *Chem. Soc. Rev.* **2014**, *43*, 99; c) A. Coskun, M. Banaszak, R. D. Astumian, J. F. Stoddart, B. A. Grzybowski, *Chem. Soc. Rev.* **2012**, *41*, 19; d) S. Silvi, M. Venturi, A. Credi, *J. Mater. Chem.* **2009**, *19*, 2279; e) W. R. Browne, B. L. Feringa, *Nat. Nanotechnol.* **2006**, *1*, 25.

[5] For recent examples see: a) P. G. Young, K. Hirose, Y. Tobe, *J. Am. Chem. Soc.* **2014**, *136*, 7899; b) C. J. Bruns, J. F. Stoddart, *Acc. Chem. Res.* **2014**, *47*, 2186; c) V. Bleve, C. Schäfer, P. Franchi, S. Silvi, E. Mezzina, A. Credi, M. Lucarini, *ChemistryOpen* **2015**, *4*, 18; d) C. Schäfer, G. Ragazzon, B. Colasson, M. La Rosa, S. Silvi, A. Credi, *ChemistryOpen*, in press, DOI: 10.1002/open.201500217.

[6] a) P. R. Ashton, I. Baxter, M. C. T. Fyfe, F. M. Raymo, N. Spencer, J. F. Stoddart, A. J. P. White, D. J. Williams, *J. Am. Chem. Soc.* **1998**, *120*, 2297; b) A. Affeld, G. M. Hubner, C. Seel, C. A. Schalley, *Eur. J. Org. Chem.* **2001**, 2877.

[7] a) M. Asakawa, P. R. Ashton, R. Ballardini, V. Balzani, M. Belohradsky, M. T. Gandolfi, O. Kocian, L. Prodi, F. M. Raymo, J. F. Stoddart, M. Venturi, *J. Am. Chem. Soc.* **1997**, *119*, 304; b) F. M. Raymo, K. N. Houk, J. F. Stoddart, *J. Am. Chem. Soc.*, **1998**, *120*, 9318; c) A. J. McConnell, P. D. Beer, *Chem. Eur. J.* **2011**, *17*, 2724.

[8] a) K. Hirose, Y. Shiba, K. Ishibashi, Y. Doi, Y. Tobe, *Chem. Eur. J.* **2008**, *14*, 981; b) Y. Tokunaga, K. Akasaka, N. Hashimoto, S. Yamanaka, K. Hisada, Y. Shimomura, S. Kakuchi, *J. Org. Chem.* **2009**, *74*, 2374; c) A. Arduini, R. Bussolati, A. Credi, S. Monaco, A. Secchi, S. Silvi, M. Venturi, *Chem. Eur. J.* **2012**, *18*, 16203; d) L.-Y. Wang, J.-L. Ko, C.-C. Lai, Y.-H. Liu, S.-M. Peng, S.-H. Chiu, *Chem. Eur. J.* **2013**, *19*, 8850.

[9] M. Baroncini, S. Silvi, M. Venturi, A. Credi, *Chem. Eur. J.* **2010**, *16*, 11580.

[10] a) R. D. Astumian, *Phys. Chem. Chem. Phys.* **2007**, *9*, 5067; b) R. D. Astumian, *Nat. Nanotechnol.* **2012**, *7*, 684.

[11] M. Baroncini, S. Silvi, M. Venturi, A. Credi, *Angew. Chem. Int. Ed.* **2012**, *51*, 4223.

[12] a) H. M. D. Bandara, S. C. Burdette, *Chem. Soc. Rev.* **2012**, *41*, 1809; b) M. Baroncini, G. Ragazzon, S. Silvi, M. Venturi, A. Credi, *Pure Appl. Chem.* **2015**, *87*, 537.

[13] G. Ragazzon, M. Baroncini, S. Silvi, M. Venturi, A. Credi, *Nat. Nanotechnol.* **2015**, *10*, 70.

[14] a) E. Sevick, *Nat. Nanotechnol.* **2015**, *10*, 18; b) G. Ragazzon, M. Baroncini, S. Silvi, M. Venturi, A. Credi, *Beilstein J. Nanotechnol.* **2015**, *6*, 2096.

[15] a) P. R. Ashton, P. J. Campbell, E. J. T. Chrystal, P. T. Glink, S. Menzer, D. Philp, N. Spencer, J. F. Stoddart, P. A. Tasker, D.J. Williams, *Angew. Chem. Int. Ed.* **1995**, *34*, 1865; b) P. R. Ashton, R. Ballardini, V. Balzani, I. Baxter, A. Credi, M. C. T. Fyfe, M. T. Gandolfi, M. Gomez-Lopez, M.-V. Martinez-Diaz, A. Piersanti, N. Spencer, J. F. Stoddart, M. Venturi, A. J. P. White, D. J. Williams, *J. Am. Chem. Soc.* **1998**, *120*, 11932.

[16] R. Car, M. Parrinello, *Phys. Rev. Lett.* **1985**, *55*, 2471.

[17] A. Laio, M. Parrinello, *Proc. Natl. Acad. Sci. U.S.A.* **2002**, *20*, 12562.

[18] a) J. W. Jones, H. W. Gibson, *J. Am. Chem. Soc.* **2003**, *125*, 7001; b) M. Clemente-Leon, C. Pasquini, V. Hebbe-Viton, J. Lacour, A. Dalla Cort, A. Credi, *Eur. J. Org. Chem.* **2006**, 105.

[19] S. Garaudée, S. Silvi, M. Venturi, A. Credi, A. H. Flood, J. F. Stoddart, ChemPhysChem 2005, 6, 2145–2152.

[20] P. Raiteri, G. Bussi, C. S. Cucinotta, A. Credi, J. F. Stoddart, M. Parrinello, *Angew. Chem. Int. Ed.* **2008**, *47*, 3536.
[21] J. P. Perdew, K. Burke, M. Ernzernhof, *Phys. Rev. Lett.* **1996**, *77*, 3865.
[22] S. Grimme, *J. Comp. Chem.* **2006**, *27*, 1787.
[23] D. Vanderbilt, *Phys Rev. B* **1990**, *41*, 7892.
[24] http://www.cpmd.org. Copyright IBM Corp. 1990-2015, MPI für Festkörperforschung Stuttgart 1997-2001.
[25] J. Tomasi, B. Mennucci, R. Cammi, *Chem. Rev.* **2005**, *105*, 2999.
[26] Gaussian 09, Revision B.01, M. J. Frisch, G. W. Trucks, H. B. Schlegel, G. E. Scuseria, M. A. Robb, J. R. Cheeseman, G. Scalmani, V. Barone, B. Mennucci, G. A. Petersson, H. Nakatsuji, M. Caricato, X. Li, H. P. Hratchian, A. F. Izmaylov, J. Bloino, G. Zheng, J. L. Sonnenberg, M. Hada, M. Ehara, K. Toyota, R. Fukuda, J. Hasegawa, M. Ishida, T. Nakajima, Y. Honda, O. Kitao, H. Nakai, T. Vreven, J. A. Montgomery, Jr., J. E. Peralta, F. Ogliaro, M. Bearpark, J. J. Heyd, E. Brothers, K. N. Kudin, V. N. Staroverov, T. Keith, R. Kobayashi, J. Normand, K. Raghavachari, A. Rendell, J. C. Burant, S. S. Iyengar, J. Tomasi, M. Cossi, N. Rega, J. M. Millam, M. Klene, J. E. Knox, J. B. Cross, V. Bakken, C. Adamo, J. Jaramillo, R. Gomperts, R. E. Stratmann, O. Yazyev, A. J. Austin, R. Cammi, C. Pomelli, J. W. Ochterski, R. L. Martin, K. Morokuma, V. G. Zakrzewski, G. A. Voth, P. Salvador, J. J. Dannenberg, S. Dapprich, A. D. Daniels, O. Farkas, J. B. Foresman, J. V. Ortiz, J. Cioslowski, D. J. Fox, Gaussian, Inc., Wallingford CT, **2010**.